PARTICLE REFLECTION IN CORRELATED COUPLING OF MONTE CARLO FORWARD-ADJOINT HISTORIES

Taro Ueki and J.E. Hoogenboom
Interfaculty Reactor Institute, Delft University of Technology
Mekelweg 15, 2629 JB Delft, The Netherlands,
Email: t.ueki@iri.tudelft.nl, j.e.hoogenboom@iri.tudelft.nl

ABSTRACT

In the rudimentary form of Monte Carlo correlated coupling, forward and adjoint histories are initiated in exactly opposite directions at an arbitrarily placed surface between a source and a detector. This methodology can be combined with a certain sort of perturbation invariance property for the surface integral of the product of directional cosine and forward and adjoint fluxes. Consequently, one is allowed to control Monte Carlo particle reflection at the aforementioned surface without introducing any bias in simulation estimators. Its significance lies in the ability of reflecting Monte Carlo particles toward the normal direction of the history-initiating surface. Particle transport along a certain direction can be enhanced. Neutral particle streaming through a long void channel is a primary candidate for the application area of such reflection control. Numerical results for two-legged duct streaming will be presented to show that the theory developed is consistent and its Monte Carlo implementation can be much more efficient than standard forward calculations.

1. INTRODUCTION

In Monte Carlo radiation transport calculations, forward and adjoint histories can be initiated in exactly opposite directions at an arbitrarily placed surface between a source and a detector, and their scores are coupled to calculate a detector response without introducing any discretization at that surface.[1] This methodology is based on the response flow integral (RFI) on a detector enclosure, which is defined as the surface integral of the product of directional cosine and forward and adjoint fluxes. The initially oppositely-moving forward and adjoint histories have exactly the same initial-state that is sampled uniformly over space and energy and isotropically over angles. Thus, the methodology may be called correlated coupling (CC), although Cramer, the original developer, did not explicitly name it. The significance of CC is that the uniform initial-state (source) sampling over all state space variables can be done at an "arbitrarily" placed intermediate surface for "any" physical source distribution function and "any" physical detector response function. This aspect of CC enables one to control the transport of "Monte Carlo" particles through the intermediate surface directly by initial-state (source) biasing.

The RFI on a physical detector enclosure has a certain sort of invariance property which is stated as follows: RFI is invariant against a perturbation in either the physical detector side volume in the forward problem or the physical source side volume in the adjoint problem. This property may be called *perturbation invariance*. Its application to Monte Carlo was first discussed by Williams with emphasis on geometric approximation,[2] and it has been employed by various Monte Carlo methodologies with both geometric and material perturbations.[3,4,5] An equivalent invariance property is summarized as "invariance for certain class of surface pseudo sources" and has been applied to forward-forward coupling calculations.[6,7] In our previous work,[8] *perturbation invariance* has been applied to CC in order to eliminate undesirable directions from initial-state (source) sampling; the directions that make both the forward and adjoint particles initially move away from their respective detector have been eliminated from the sampling of the angle coordinate vector of initial states, by the perturbation with a black absorber or a reverse and mirror reflecting material. The resulting CC has been shown to be much more efficient than the rudimentary CC by Cramer.

In this work, we generalize the CC with reflection perturbation by incorporating reflection "fairly" biased toward the normal direction of an intermediate surface. If that surface is placed inside a void channel and the normal direction agrees with the axial direction of the channel, the generalized CC should enhance Monte Carlo particle's streaming through the void. This can be considered a fair Monte Carlo game with reflection control at a surface strictly inside void. Numerical results for two-legged duct streaming will be presented to show the correctness of the related theoretical analysis and the efficiency of its CC implementation.

2. THEORY

In principle CC can be implemented in continuous energy Monte Carlo.[8] However, for notational convenience and the fact that general purpose continuous energy adjoint options are not commonly used,[9] the theory of CC is described in multigroup energy framework. We consider a perturbed forward problem for a source-detector system in a domain $V = V_F \bigcup V_A$:

$$\begin{aligned}&\underline{\Omega} \cdot \underline{\nabla}\check{\psi}_g(\underline{r}, \underline{\Omega}) + \Sigma_{t,g}(\underline{r})\check{\psi}_g(\underline{r}, \underline{\Omega}) \\ &\qquad = \sum_{g'=1}^{G} \int_{4\pi} \Sigma_{s,g'\to g}(\underline{r}, \underline{\Omega}' \to \underline{\Omega})\check{\psi}_{g'}(\underline{r}, \underline{\Omega}')d\Omega' + S_g^F(\underline{r}, \underline{\Omega}) \text{ for } \underline{r} \in V_F,\end{aligned} \tag{1}$$

$$\underline{\Omega} \cdot \underline{\nabla}\check{\psi}_g(\underline{r}, \underline{\Omega}) + \check{\Sigma}_{t,g}(\underline{r}, \underline{\Omega})\check{\psi}_g(\underline{r}, \underline{\Omega}) = \sum_{g'=1}^{G} \int_{4\pi} \check{\Sigma}_{s,g'\to g}(\underline{r}, \underline{\Omega}' \to \underline{\Omega})\check{\psi}_{g'}(\underline{r}, \underline{\Omega}')d\Omega' \text{ for } \underline{r} \in V_A\ , \tag{2}$$

$$\check{\psi}_g(\underline{r}, \underline{\Omega}) = 0 \qquad \text{for } \underline{r} \in \partial V \text{ and } \underline{\Omega} \cdot \underline{n} < 0, \tag{3}$$

and an unperturbed adjoint problem for the same system:

$$-\underline{\Omega} \cdot \underline{\nabla}\psi_g^*(\underline{r}, \underline{\Omega}) + \Sigma_{t,g}(\underline{r})\psi_g^*(\underline{r}, \underline{\Omega})$$
$$= \sum_{g'=1}^{G} \int_{4\pi} \Sigma_{s,g\to g'}(\underline{r}, \underline{\Omega} \to \underline{\Omega}')\psi_{g'}^*(\underline{r}, \underline{\Omega}')d\Omega' + S_g^A(\underline{r}, \underline{\Omega}) \text{ for } \underline{r} \in V, \quad (4)$$
$$\psi_g^*(\underline{r}, \underline{\Omega}) = 0 \text{ for } \underline{r} \in \partial V \text{ and } \underline{\Omega} \cdot \underline{n} > 0, \quad (5)$$

where the check $(\check{\cdot})$ in the forward problem stands for perturbed quantities, V_A and V_F are

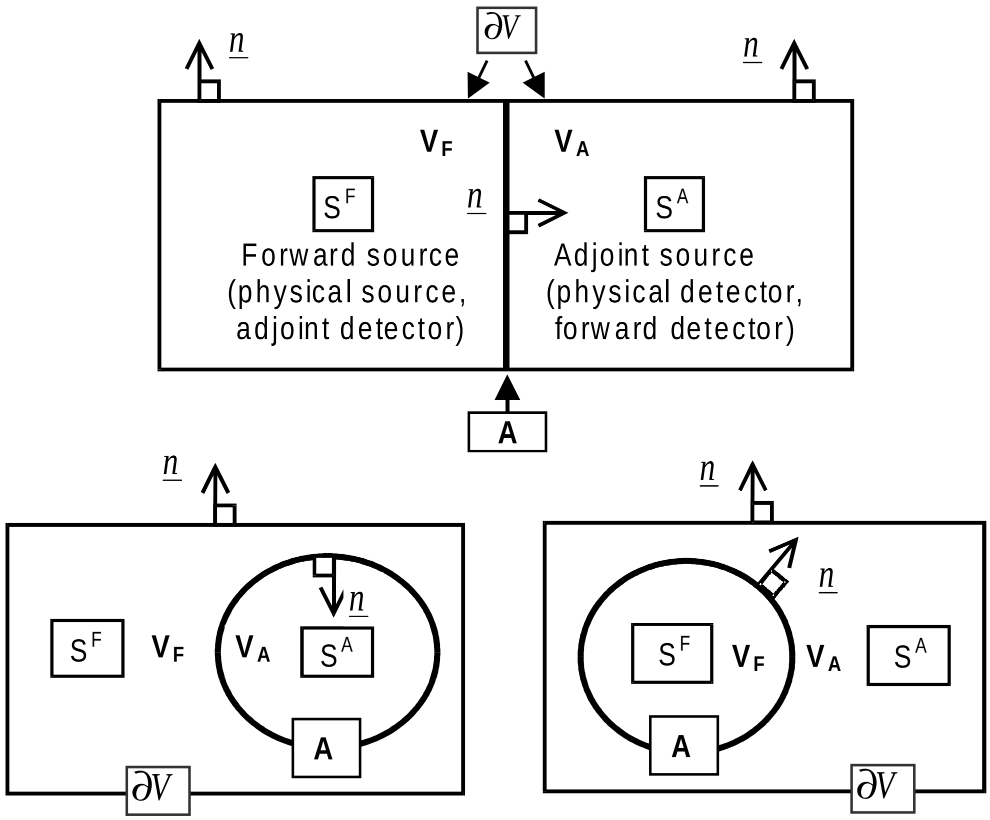

Figure 1: Enclosure set-ups in source-detector system

respectively the detector and source side volumes separated by the intermediate surface A $(= \partial V_A \bigcap \partial V_F)$ whose positive side is the detector side volume, ∂V is the exterior boundary, S_g^F the physical source distribution function, S_g^A the physical detector response function, and other notations are standard. Also, it is assumed that $S_g^F = 0$ in V_A and $S_g^A = 0$ in V_F. See figure 1. In Eqs. (1)-(3), macroscopic cross sections are perturbed only in V_A, but the forward flux is perturbed throughout the whole spatial domain. In other words, the local perturbation of macroscopic cross sections globally perturbs the forward flux. By the *perturbation invariance* that is stated in the previous section, the detector response R of the unperturbed physical problem represented by Eqs. (4)-(5) has two expressions in terms of the perturbed forward and unperturbed adjoint fluxes:

$$R = \sum_{g=1}^{G} \int_{V_F} \int_{4\pi} S_g^F(\underline{r}, \Omega)\psi_g^*(\underline{r}, \Omega) d\Omega dV = \sum_{g=1}^{G} \int_A \int_{4\pi} \underline{n} \cdot \Omega \check{\psi}_g(\underline{r}, \Omega)\psi_g^*(\underline{r}, \Omega) d\Omega dA \,. \tag{6}$$

[The second equality can be derived by considering that in the physical source side volume (V_F), $S_g^A = 0$ and the transport operators in the perturbed forward and unperturbed adjoint problems are formally adjoint to each other. Here, the transport operators stand for the sum of the streaming and collision terms subtracted by the scattering terms. Recall that the macroscopic cross sections are not perturbed in V_F.] In Eq. (6), the first equality always holds, while the second equality is valid only when the intermediate surface A is set up as in figure 1. The physical meaning of the second equality of Eq. (6) can be interpreted based on a black absorber perturbation as a reference perturbation.[8]

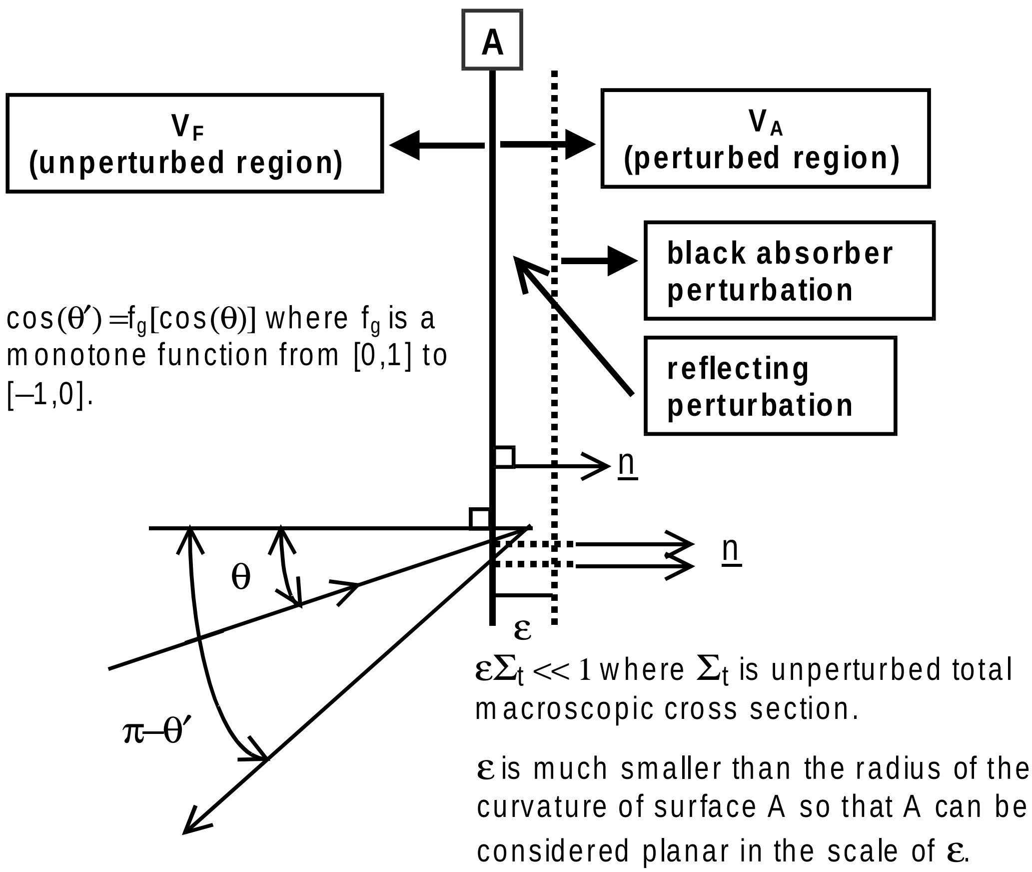

Figure 2: Perturbation for reflection control

At position $\underline{r}$ on the surface A, the polar angle θ with respect to and the azimuthal angle ϕ around $\underline{n}(\underline{r})$ are defined. We then consider a perturbation with the scattering from the precollision directional cosine $\mu = \cos(\theta) = \underline{n} \cdot \underline{\Omega}$ to the postcollision directional cosine

$\mu' = \underline{n} \cdot \underline{\Omega}' = f_g(\mu)$ (< 0) and with the precollision angle dependent multiplicative factor $h_g(\mu)$, in a sufficiently thin layer in V_A with thickness ϵ adjacent to A:

$$\check{\Sigma}_{t,g}(\underline{r}, \underline{\Omega}) = \begin{cases} \check{\Sigma}^+_{t,g} & \text{for } \underline{n} \cdot \underline{\Omega} > 0 \\ \check{\Sigma}^-_{t,g} & \text{for } \underline{n} \cdot \underline{\Omega} < 0 \end{cases}, \tag{7}$$

$$\check{\Sigma}_{s,g\to g'}(\underline{r}, \underline{\Omega} \to \underline{\Omega}') = \begin{cases} \check{\Sigma}^+_{t,g}\delta_{g',g}h_g(\mu)\delta[f_g(\mu) - \mu']\delta(\phi + \pi - \phi') & \text{for } \underline{n} \cdot \underline{\Omega} > 0 \\ \check{\Sigma}^-_{t,g}\delta_{g',g}\delta(\mu - \mu')\delta(\phi - \phi') & \text{for } \underline{n} \cdot \underline{\Omega} < 0 \end{cases}. \tag{8}$$

In the above, $\underline{n}$ is defined at the intersection closer to $\underline{r}$ of A and $\underline{r} + s\underline{\Omega}$, $-\infty < s < \infty$, $f_g(\mu)$ is assumed to be a monotone and differentiable function of μ which maps $[0, 1]$ to $[-1, 0]$. The assumptions about $f_g(\mu)$ are due to technical reasons which will be stated at appropriate derivation steps. $h_g(\mu)$ has been introduced as extra freedom which will play a role in Monte Carlo simulations. When a particle enters the perturbed region through A, the first collision process represented by Eqs. (7) and (8) uniquely changes (μ, ϕ) to $(f_g(\mu), \phi+\pi)$ with no energy change, and the mean number of particles emerging from that collision is $h_g(\mu)$. Once a particle survives the first collision, it is certain to travel to the surface A with no change in both the direction and energy. Figure 2 explains such a process together with a black absorber perturbation in V_A except the thin layer adjacent to A. A black absorber perturbation can be treated by a purely absorbing material with the total macroscopic cross section tending to infinity.

As a next step we take $\check{\Sigma}^+_{t,g}$ to infinity while keeping $\check{\Sigma}^-_{t,g}$ finite and fixed. We then express the limit of $\check{\psi}_g(\underline{r}, \underline{\Omega})$ in V_F by $\check{\eta}_g(\underline{r}, \underline{\Omega})$:

$$\check{\eta}_g(\underline{r}, \underline{\Omega}) \equiv \lim_{\check{\Sigma}^+_{t,g}\to\infty} \check{\psi}_g(\underline{r}, \underline{\Omega}) \text{ for } \underline{r} \in V_F. \tag{9}$$

The perturbation by Eqs. (7) and (8) dictates that the reflecting angular differential current through the unit area on A, $-f_g(\mu)\check{\eta}_g[\underline{r}, f_g(\mu), \phi + \pi]\,|d[f_g(\mu)]|\,d(\phi + \pi)$, is equal to the impinging angular differential current through the same unit area on A, $\mu\check{\eta}_g(\underline{r}, \mu, \phi)|d\mu|d\phi$, multiplied by the multiplicative factor $h_g(\mu)$:

$$-f_g(\mu)\check{\eta}_g[\underline{r}, f_g(\mu), \phi + \pi]\,|d[f_g(\mu)]|\,d(\phi + \pi) = h_g(\mu)\mu\check{\eta}_g(\underline{r}, \mu, \phi)|d\mu|d\phi,\ \underline{r} \in A,\ 0 < \mu < 1. \tag{10}$$

The monotonicity and differentiability of $f_g(\mu)$ have been introduced for this treatment to be valid. $\check{\eta}_g(\underline{r}, \mu, \phi)$ is then the solution of the following forward problem:

$$\begin{aligned} &\underline{\Omega} \cdot \underline{\nabla}\check{\eta}_g(\underline{r}, \underline{\Omega}) + \Sigma_{t,g}(\underline{r})\check{\eta}_g(\underline{r}, \underline{\Omega}) \\ &\quad = \sum_{g'=1}^{G} \int_{4\pi} \Sigma_{s,g'\to g}(\underline{r}, \underline{\Omega}' \to \underline{\Omega})\check{\eta}_{g'}(\underline{r}, \underline{\Omega}')d\Omega' + S^F_g(\underline{r}, \underline{\Omega}) \text{ for } \underline{r} \in V_F, \end{aligned} \tag{11}$$

$$-\frac{f_g(\mu)}{h_g(\mu)\mu}\left|\frac{df_g(\mu)}{d\mu}\right|\check{\eta}_g[\underline{r}, f_g(\mu), \phi + \pi] = \check{\eta}_g(\underline{r}, \mu, \phi) \text{ for } \underline{r} \in A \text{ and } \mu > 0, \tag{12}$$

$$\check{\eta}_g(\underline{r}, \underline{\Omega}) = 0 \text{ for } \underline{r} \in \partial V \textstyle\bigcap \partial V_F \text{ and } \underline{\Omega} \cdot \underline{n} < 0. \tag{13}$$

Here, $-1 \leq f_g(\mu) \leq 0$ in Eq. (12), Eq. (13) is relevant only when the upper and lower-left drawings are concerned ($\partial V \bigcap \partial V_F$ is an empty set for the lower-right drawing in figure 1), and the 2π-periodicity of ϕ is assumed for $\check{\eta}_g$. Since $f_g(\mu)$ is a monotone function of μ from $[0,1]$ to $[-1,0]$, Eq. (12) specifies the boundary condition on A.

Rigorously speaking, Eq. (10) with $\check{\eta}_g$ replaced by $\check{\psi}_g$ should be derived by asymptotic analysis with $\check{\Sigma}^+_{t,g} \to \infty$, which enables one to make the definition in (9) with Eqs. (11)-(13). This must await future study.

By the *perturbation invariance*, the RFI, the third term in Eq. (6), is equal to the detector response for any non-negative values of $\check{\Sigma}^+_{t,g}$. Therefore, we obtain:

$$\begin{aligned} R &= \lim_{\check{\Sigma}^+_{t,g} \to \infty} \sum_{g=1}^{G} \int_A \int_{4\pi} \underline{n} \cdot \underline{\Omega}' \check{\psi}_g(\underline{r}, \underline{\Omega}') \psi^*_g(\underline{r}, \underline{\Omega}') d\Omega' dA \\ &= \sum_{g=1}^{G} \int_A \int_{4\pi} \underline{n} \cdot \underline{\Omega}' \check{\eta}_g(\underline{r}, \underline{\Omega}') \psi^*_g(\underline{r}, \underline{\Omega}') d\Omega' dA, \end{aligned} \tag{14}$$

where we have interchanged the order of the integral and limit and have used the definition in (9). If $\check{\psi}_g(\underline{r}, \underline{\Omega})$ is dominated (bounded above) by an integrable function, the dominated convergence theorem allows one to do such interchange.[10,11] Again, asymptotic analysis would be required to show the boundedness during the limit process. Rigorous mathematical treatments of such an aspect must await future study.

The angle integral in Eq. (14) is separated into the $\underline{n} \cdot \underline{\Omega}' > 0$ and $\underline{n} \cdot \underline{\Omega}' < 0$ domains. In the integral corresponding to the latter domain, the angle integration variables are changed from ϕ' to $\phi = \phi' - \pi$ and from μ' to $\mu = f_g^{-1}(\mu')$, where $f_g^{-1}(\mu)$ is the inverse of $f_g(\mu)$: $\mu' = f_g(\mu)$. $df_g(\mu)/d\mu$ is positive when $f_g(\mu)$ is an increasing function of μ, and $df_g(\mu)/d\mu$ is negative when $f_g(\mu)$ is a decreasing function of μ. Thus, Eq. (10) allows one to rewrite Eq. (14) as

$$R = \sum_{g=1}^{G} \int_A \int_0^{2\pi} \int_0^1 \check{\eta}_g(\underline{r}, \mu, \phi) [\psi^*_g(\underline{r}, \mu, \phi) - h_g(\mu) \psi^*_g(\underline{r}, f_g(\mu), \phi + \pi)] \, \mu \, d\mu d\phi dA \, . \tag{15}$$

We rewrite the right hand side of Eq. (15) as

$$\begin{aligned} \pi \mathcal{A} G \sum_{g=1}^{G} \frac{1}{G} \int_A \int_0^{2\pi} \int_0^1 & \check{\eta}_g(\underline{r}, \mu, \phi) \\ & \times \left[\psi^*_g(\underline{r}, \mu, \phi) - h_g(\mu) \psi^*_g(\underline{r}, f_g(\mu), \phi + \pi) \right] \frac{\mu d\mu d\phi}{\pi} \frac{dA}{\mathcal{A}}, \; \mathcal{A} = \textstyle\int_A dA, \end{aligned} \tag{16}$$

and consider $\mu / \pi \mathcal{A} G$ as the probability density function that is uniform over energy, space (on surface A) and azimuthal angles, and cosine-distributed over the positive half of polar angles. (Note that $\sum_{g=1}^{G} \int_A \int_0^1 \int_0^{2\pi} \mu / (\pi \mathcal{A} G) d\phi d\mu dA = 1$.) Suppose that source variables sampled from the above density function are $(g_0, \underline{r}_0, \mu_0, \phi_0)$ for energy group g, position $\underline{r}$, polar angle μ and azimuthal angle ϕ. Here, $(g_0, \underline{r}_0, \mu_0, \phi_0)$ represents an initial state for independently-replicated stochastic experiments. The task to be done is to estimate:

$$\check{\eta}_{g_0}(\underline{r}_0, \mu_0, \phi_0)\left[\psi^*_{g_0}(\underline{r}_0, \mu_0, \phi_0) - h_{g_0}(\mu_0)\psi^*_{g_0}(\underline{r}_0, f_{g_0}(\mu_0), \phi_0 + \pi)\right]. \quad (17)$$

Conditioned on the realized initial state $(g_0, \underline{r}_0, \mu_0, \phi_0)$, we construct three independent transport problems to calculate $\check{\eta}_{g_0}(\underline{r}_0, \mu_0, \phi_0)$, $\psi^*_{g_0}(\underline{r}_0, \mu_0, \phi_0)$ and $\psi^*_{g_0}[\underline{r}_0, f_{g_0}(\mu_0), \phi_0 + \pi]$. An important concept involved is conditional independence: once $(g_0, \underline{r}_0, \mu_0, \phi_0)$ is fixed, the simulations for these three quantities can be done independently. In other words, the independently-replicated stochastic experiments consist of three independent Monte Carlo simulations conditional on the initial state. The following quantity then becomes a statistical entity for the detector response calculation:

$$\begin{aligned}&[\text{Monte Carlo score for } \check{\eta}_{g_0}(\underline{r}_0, \mu_0, \phi_0)] \times \Big\{\left[\text{Monte Carlo score for } \psi^*_{g_0}(\underline{r}_0, \mu_0, \phi_0)\right] \\ &\quad - h_{g_0}(\mu_0)\left[\text{Monte Carlo score for } \psi^*_{g_0}(\underline{r}_0, f_{g_0}(\mu_0), \phi_0 + \pi)\right]\Big\}. \quad (18)\end{aligned}$$

The normalization constant is $\pi\mathcal{A}G$. The conditional independence ensures that the expected value of Eq. (18) assuming the realization $(g_0, \underline{r}_0, \mu_0, \phi_0)$ is equal to Eq. (17). Here, it is implicitly supposed that there exists an unbiased simulation for each of the estimations of the three fluxes in Eq. (17). If the formally adjoint transport problems are appropriately formulated, standard forward and adjoint simulations give one unbiased estimations of these fluxes. How to formulate such transport problems will be stated later. Other important concept is that the expected value of a conditional expectation under a given set of stochastic rules is equal to the true expected value under the same set of stochastic rules. (Simply put, the expected value of a conditional expectation is a true expectation. See reference 11 for rigorous mathematical derivation of this relation) Since the initial state $(g_0, \underline{r}_0, \mu_0, \phi_0)$ is independently sampled from the probability density function $\mu/(\pi\mathcal{A}G)$, Eq. (18) multiplied by $\pi\mathcal{A}G$ is an unbiased estimate of the detector response R. All the foregoing discussions are required because in general the expected value of the product of random variables is not equal to the product of the expected values of the same random variables.

The forward flux $\check{\eta}_{g_0}(\underline{r}_0, \mu_0, \phi_0)$ is estimated by simulating a formally adjoint problem whose solution is denoted by $\check{\eta}^*_g$. To formulate that adjoint problem, we have to take care of the subtlety residing in expressing a point source at $\underline{r}_0 \in A$. The boundary condition on A is decomposed into $\check{\eta}^{*,r}_g$ and $\check{\eta}^{*,ur}_g$ which are components due to adjoint particles which have and have not reflected at A; $\check{\eta}^*_g = \check{\eta}^{*,r}_g + \check{\eta}^{*,ur}_g$. δ_A, the Dirac delta function on the surface A; $\int_A F_A(\underline{r})\delta_A(\underline{r} - \underline{r}_0)dA = F_A(\underline{r}_0)$ for functions F_A on A, is used to specify the boundary condition of $\check{\eta}^{*,ur}_g$. Such treatments are similar to expressing a point source on the convex external surface with vacuum boundary condition according to collided and uncollided components.[12] The resulting adjoint equation becomes:

$$-\underline{\Omega} \cdot \underline{\nabla}\check{\eta}^*_g(\underline{r}, \underline{\Omega}) + \Sigma_{t,g}(\underline{r})\check{\eta}^*_g(\underline{r}, \underline{\Omega}) = \sum_{g'=1}^{G} \int_{4\pi} \Sigma_{s,g\to g'}(\underline{r}, \underline{\Omega} \to \underline{\Omega}')\check{\eta}^*_{g'}(\underline{r}, \underline{\Omega}')d\Omega' \text{ for } \underline{r} \in V_F, \quad (19)$$

$$\check{\eta}_g^{*,ur}(\underline{r},\mu,\phi)=\delta_{g,g0}\delta_A(\underline{r}-\underline{r}_0)\delta(\mu-\mu_0)\delta(\phi-\phi_0)\;/\;\mu_0 \text{ for } \underline{r}\in A \text{ and } \mu>0, \tag{20}$$

$$\check{\eta}_g^{*,r}(\underline{r},\mu,\phi)=h_g(\mu)\check{\eta}_g^*[\underline{r},f_g(\mu),\phi+\pi] \text{ for } \underline{r}\in A \text{ and } \mu>0, \tag{21}$$

$$\check{\eta}_g^*(\underline{r},\underline{\Omega})=0 \text{ for } \underline{r}\in\partial V\cap\partial V_F \text{ and } \underline{\Omega}\cdot\underline{n}>0, \tag{22}$$

where the 2π periodicity of ϕ is assumed for $\check{\eta}_g^*$ on A, and Eq. (22) is not relevant for the lower-right drawing in figure 1, for which $\partial V\cap\partial V_F$ is an empty set. Recall also that adjoint particles move in directions opposite to the angle coordinate vector of the state space variables.

Now, we explain the boundary condition in Eq. (21). Eq. (12) combined with Eq. (21) yield

$$\begin{aligned}&\mu\check{\eta}_g(\underline{r},\mu,\phi)\check{\eta}_g^{*,r}(\underline{r},\mu,\phi)|d\mu|d\phi\\&=-f_g(\mu)\check{\eta}_g[\underline{r},f_g(\mu),\phi+\pi]\check{\eta}_g^*[\underline{r},f_g(\mu),\phi+\pi]|df_g(\mu)|d(\phi+\pi) \text{ for } \underline{r}\in A \text{ and } \mu>0.\end{aligned} \tag{23}$$

This relation leads to

$$\begin{aligned}&\sum_{g=1}^{G}\int_A\int_0^1\int_{2\pi}\underline{n}\cdot\underline{\Omega}\check{\eta}_g(\underline{r},\mu,\phi)\check{\eta}_g^{*,r}(\underline{r},\mu,\phi)d\phi d\mu dA\\&=-\sum_{g=1}^{G}\int_A\int_{-1}^0\int_{2\pi}\underline{n}\cdot\underline{\Omega}\check{\eta}_g(\underline{r},\mu,\phi)\check{\eta}_g^*(\underline{r},\mu,\phi)d\phi d\mu dA.\end{aligned} \tag{24}$$

Therefore, Eqs. (11)-(13) and (19)-(22) yield

$$\check{\eta}_{g0}(\underline{r}_0,\mu_0,\phi_0)=\sum_{g=1}^{G}\int_{V_F}\int_{4\pi}S_g^F(\underline{r},\underline{\Omega})\check{\eta}_g^*(\underline{r},\underline{\Omega})d\Omega dV. \tag{25}$$

This relation ensures that the unbiased Monte Carlo simulation of Eqs. (19)-(22) gives a correct answer to the estimation of $\check{\eta}_{g0}(\underline{r}_0,\mu_0,\phi_0)$. Eq. (21) is rewritten as

$$\begin{aligned}&\mu\check{\eta}_g^{*,r}(\underline{r},\mu,\phi)|d\mu|d\phi=\\&-\left|\frac{\mu h_g(\mu)}{f_g(\mu)}\right|\left|\frac{df_g(\mu)}{d\mu}\right|^{-1}f_g(\mu)\check{\eta}_g^*[\underline{r},f_g(\mu),\phi+\pi]|d[f_g(\mu)]|d(\phi+\pi) \text{ for } \underline{r}\in A \text{ and } \mu>0.\end{aligned} \tag{26}$$

Since $\mu\check{\eta}_g^{*,r}(\underline{r},\mu,\phi)|d\mu|d\phi$ is the reflecting adjoint angular differential current through the unit area on A and $-f_g(\mu)\check{\eta}_g^*[\underline{r},f_g(\mu),\phi+\pi]|d[f_g(\mu)]|d(\phi+\pi)$ is the impinging adjoint angular differential current through the same unit area on A, Eq. (26) implies that the weight correction factor at the reflection is $|\mu h_g(\mu)/f_g(\mu)|\,|df_g(\mu)/d\mu|^{-1}$. Recall again that adjoint particles move in directions opposite to the angle coordinate vector $\underline{\Omega}$ of the state space variables.

We choose $f_g(\mu)$ as

$$f_g(\mu)=-\mu^{p_g} \text{ with } p_g\geq 1 \text{ for } \mu>0. \tag{27}$$

This implies

direction cosine before reflection: $-\mu(<0)\Rightarrow$ direction cosine after reflection: μ^{1/p_g}.

Therefore, adjoint particles are reflected toward the normal direction of the surface A.

We choose $h_g(\mu)$ as

$$h_g(\mu) = q_g \mu^{2p_g-2}. \tag{28}$$

This implies that the weight correction factor is angle-independent:

$$\left|\frac{\mu h_g(\mu)}{f_g(\mu)}\right| \left|\frac{df_g(\mu)}{d\mu}\right|^{-1} = \frac{q_g}{p_g}.$$

The unperturbed adjoint flux $\psi^*_{g0}(\underline{r}_0, \mu_0, \phi_0)$ is estimated by the unbiased Monte Carlo simulation of the following unperturbed forward problem:

$$\underline{\Omega} \cdot \underline{\nabla}\psi_g(\underline{r}, \underline{\Omega}) + \Sigma_{t,g}(\underline{r})\psi_g(\underline{r}, \underline{\Omega}) = \sum_{g'=1}^{G} \int_{4\pi} \Sigma_{s,g'\to g}(\underline{r}, \underline{\Omega}' \to \underline{\Omega})\psi_{g'}(\underline{r}, \underline{\Omega}')d\Omega'$$
$$+\delta_{g,g0}\delta(\underline{r} - \underline{r}_0)\delta(\mu - \mu_0)\delta(\phi - \phi_0) \text{ for } \underline{r} \in V, \tag{29}$$
$$\psi_g(\underline{r}, \underline{\Omega}) = 0 \text{ for } \underline{r} \in \partial V \text{ and } \underline{\Omega} \cdot \underline{n} < 0. \tag{30}$$

The unperturbed adjoint flux $\psi^*_{g0}[\underline{r}_0, f_{g0}(\mu_0), \phi_0 + \pi]$ is estimated by the unbiased Monte Carlo simulation of Eqs (29)-(30) with the source $\delta_{g,g0}\delta(\underline{r} - \underline{r}_0)\delta(\mu - \mu_0)\delta(\phi - \phi_0)$ replaced by $\delta_{g,g0}\delta(\underline{r} - \underline{r}_0)\delta[\mu - f_{g0}(\mu_0)]\delta(\phi - \phi_0 - \pi)$.

3. NUMERICAL RESULTS

We show numerical results for two-legged duct streaming with seven group macroscopic cross sections. The centerlines of both duct-legs are 50 cm in length. They form a right angle. The void cross-sectional area is a square with 10 cm sides. The wall thickness is 10 cm. No particle transport is assumed for the material outside the wall. A spatially-uniform physical plane-source for the first (highest energy) group with inward-cosine distribution in polar angles and uniform distribution in azimuthal angles is placed normal to the duct centerline inside the void at the end of the one leg, and flux spectra are calculated at the void exit at the end of the other leg. The surface A is placed as shown in figure 3. Initial-state (source) sampling for CC is done on A. The macroscopic cross section data in cm^{-1} are: $\Sigma_{t,g} = 0.30$, 0.32, 0.34, 0.37, 0.45, 0.55, 0.65, $\Sigma_{s,g} = 0.28$, 0.30, 0.32, 0.35, 0.43, 0.53, 0.63 for $g = 1, \cdots 7$, $\Sigma_{s,1\to 2} = 0.14$, $\Sigma_{s,1\to 3} = 0.056$, $\Sigma_{s,2\to 3} = 0.15$, $\Sigma_{s,2\to 4} = 0.06$, $\Sigma_{s,3\to 4} = 0.16$, $\Sigma_{s,3\to 5} = 0.064$, $\Sigma_{s,4\to 5} = 0.21$, $\Sigma_{s,5\to 6} = 0.215$, $\Sigma_{s,6\to 7} = 0.265$, ($\Sigma_{s,7\to 8} = 0.315$). Scattering is isotropic and no upscattering is assumed. These values are intended to capture the properties of highly scattering material.

Results for CC with $p_1 = 20$, $q_1 = 1$, and $p_g = q_g = 2$, $g = 2, \ldots, 7$ are shown with those from standard forward calculations in table 1. In CC, initial-state (source) biasing was employed following the procedures described in reference 8. For any physical source

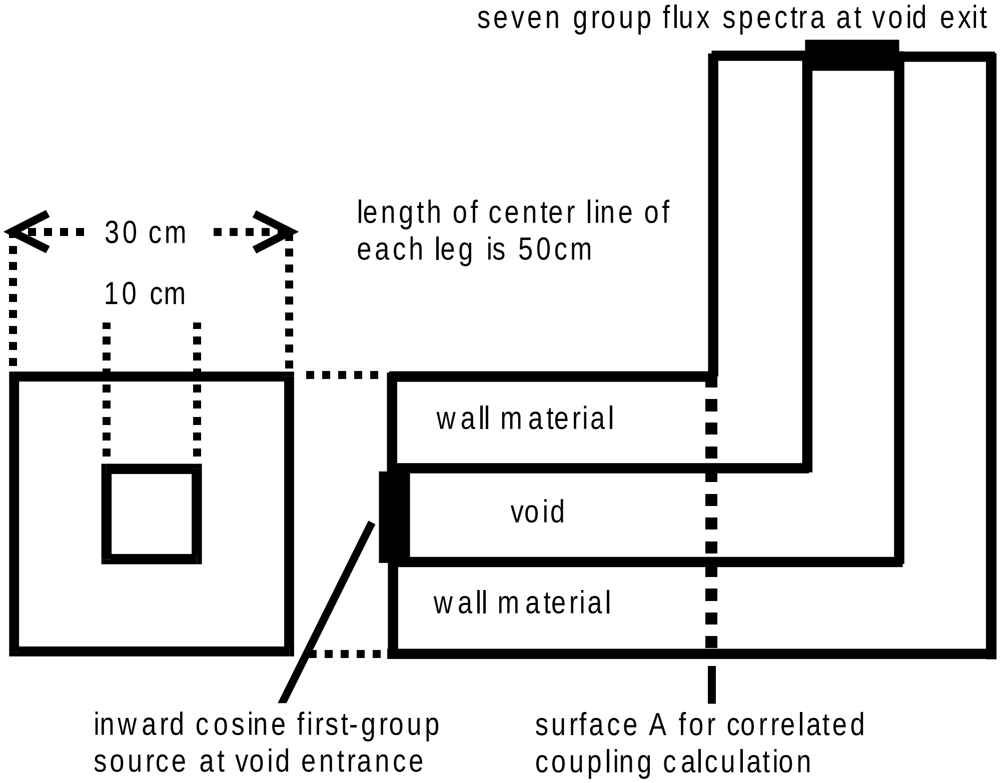

Figure 3: Two legged duct streaming problem (no particle transport is assumed for the region outside wall)

Table 1: Seven group flux spectra at void exit per physical source particle

Standard forward, 6,000,000,000 histories, cpu time = 2886 min.$^{a)}$						
1st	2nd	3rd	4th	5th	6th	7th
4.937e-8 (0.62%)	1.071e-7 (0.43%)	1.070e-7 (0.46%)	1.032e-7 (0.49%)	1.270e-7 (0.46%)	1.021e-7 (0.52%)	8.457e-8 (0.60%)
CC, 2,000,000,000 initial-state (source) samplings; 3 adjoint and (2 $\times$) 30 forward histories per initial-state, cpu time = 1783 min.$^{a)}$						
1st	2nd	3rd	4th	5th	6th	7th
4.980e-8 (0.40%)	1.084e-7 (0.29%)	1.059e-7 (0.32%)	1.028e-7 (0.38%)	1.258e-7 (0.39%)	1.022e-7 (0.53%)	8.464e-8 (0.57%)

a) cpu time was measured by Digital AlphaStation 600 5 distribution function and any physical detector response funtion, the initial-state (source) sampling described in the previous section is valid. In other words, great freedom is always given to initial-state (source) sampling through the uniform probability density function over the whole area of the surface A and the entire energy range of a given physical problem . We have exploited such freedom. Void-surface to non-void-surface biased spatial density ratio is set to ten. This is because the particle flux could vary by an order of magnitude between void and non-void parts. Biased energy density ratio is 8:4:2:1:1:1:0.5 from the first to the seven energy group. This is because no physical (forward) upscattering is allowed in this problem. The reflecting perturbation is employed only for the void part of the surface A. In the non-void part of surface A, a black absorber perturbation without a thin reflecting layer was employed. Thus, when adjoint particles return to the non-void part of A, they are terminated, while when they return to the void part of A, they are reflected according to Eq. (26). Also, when the space coordinate of the initial state $\underline{r_0}$ belongs to the non-void part of A, the forward simulation for estimating $\psi^*_{g0}[\underline{r}_0, f_{g0}(\mu_0), \phi_0 + \pi]$ is not performed. We used a random number generator with a long period ($\approx 10^{18}$) constructed from two algorithmically quite different generators in reference 13. We also used batch-average product processing[8]. This is because the non-zero probability of the coupled-score [Eq. (18) $\times\ \pi G\mathcal{A}$] increases quadratically as the forward and adjoint batch sizes increase, which outweights the linear increase of cpu time. In table 1, CC appears to be very efficient. This efficiency gain has been obtained without transport biasing like space-energy-angle dependent Russian roulette and splitting games. When all histories in the adjoint batch for a selected initial state yield a zero score, there is no corresponding forward simulation (the coupled score is zero; zero multiplied by a real number always becomes zero) and we proceed to the sampling of the next initial state. In addition, the scattering probability for first group adjoint particles is usually small. In many cases, these two aspects lead to short cpu time for CC.

4. CONCLUSIONS AND DISCUSSION

A perturbation invariance property of the surface integral of the product of directional cosine and forward and adjoint fluxes has been combined with Monte Carlo correlated coupling (CC). Consequently, one can control the particle reflection at an arbitrarily placed surface between a source and a detector. Numerical results for two-legged duct streaming show that CC can be very efficient. Actually, initial-state (source) biasing was employed in CC. However, such biasing is not a disadvantage to CC because the initial-state (source) distribution is always uniform over space, energy and azimuthal angles, and cosine-distributed over polar angles, for any physical source distribution function and any physical detector response function.

A power form of the cosine of polar angles has been employed for the reflection control. However, that form is not the only possibility. Moreover, we may be able to relax the assumption made on the functional of polar angles. For azimuthal angles, the rudimentary reversing control (the addition of π) has been tried. It is certainly possible to explore more sophisticated functional of azimuthal angles. All those analyses must await future study.

REFERENCES

1. S.N. Cramer, "Forward-Adjoint Monte Carlo Coupling with No Statistical Error Propagation," *Nucl. Sci. Eng.* **124**, 398, (1996).

2. M.L. Williams, "Generalized Contributon Response Theory," *Nucl. Sci. Eng.* **108**, 355, (1991).

3. C.H. Aboughantous, "A Contributon Monte Carlo Method," *Nucl. Sci. Eng.* **118**, 160, (1994).

4. I.V. Serov, T.M. John and J.E. Hoogenboom, "A Midway Forward-Adjoint Coupling Method for Neutron and Photon Monte Carlo Transport," *Nucl. Sci. Eng.* **133**, 55 (1999).

5. T. Ueki, J.E. Hoogenboom and J.L. Kloosterman, "Monte Carlo Forward-Adjoint Coupling by Next Event Estimation," in proceedings of *Mathematics and Computation, Reactor Physics and Environmental Analysis in Nuclear Applications*, Vol. 1, p.241, Madrid Spain, September 27-30 (1999).

6. V.V. Korobejnikov and V.I. Oussanov, *Invariance for Certain Class of Surface Pseudo Sources*, (in Russian) Preprint IPPE-2080, Obninsk, (1990).

7. V.V. Korobejnikov, V.A. Grabejnoi, V.I. Oussanov, L.P. Bass, and A.N. Khmyljev, "Application of the Combined Method for Neutron Transport Calculations in Three Dimensional Systems," in proceedings of the *Joint International Conference on Mathematical Methods and Supercomputing for Nuclear Applications*, Vol. 1, p.713, Saratoga Springs, New York U.S.A., October 5-9 (1997).

8. T. Ueki, J.E. Hoogenboom and J.L. Kloosterman, "Analysis of Correlated Coupling of Monte Carlo Forward and Adjoint Histories," *Nucl. Sci. Eng.,* submitted.

9. J.E. Hoogenboom, "Continuous Energy Adjoint Monte Carlo in MCNP with Minor Code Extensions," in proceedings of *Mathematics and Computation, Reactor Physics and Environmental Analysis in Nuclear Applications*, Vol. 2 p.1762 in book proceedings (p.1912 in CD proceedings), Madrid Spain, September 27-30 (1999).

10. G.B. Folland, *Real Analysis*, Second Edition, John Wiley & Sons, New York U.S.A. (1999).

11. P. Billingsley, *Probability and Measure*, Third Edition, John Wiley & Sons, New York U.S.A. (1995).

12. R. Sánchez, "Duality, Green's Functions and all that," *Transport Theory and Statistical Physics* **27**(5-7), 445 (1998).

13. W.H. Press, S.A. Teukolsky, W.T. Vetterling and B.P. Flannery, *Numerical Recipes in Fortran 90*, Cambridge University Press, New York U.S.A. (1996)